Fiducial Optimization for Minimal Target Registration Error in Image-Guided Neurosurgery

Reuben R. Shamir*, *Member, IEEE*, Leo Joskowicz, *Senior Member, IEEE*, and Yigal Shoshan

***Abstract*—This paper presents new methods for the optimal selection of anatomical landmarks and optimal placement of fiducial markers in image-guided neurosurgery. These methods allow the surgeon to optimally plan fiducial marker locations on routine diagnostic images before preoperative imaging and to intraoperatively select the set of fiducial markers and anatomical landmarks that minimize the expected target registration error (TRE). The optimization relies on a novel empirical simulation-based TRE estimation method built on actual fiducial localization error (FLE) data. Our methods take the guesswork out of the registration process and can reduce localization error without additional imaging and hardware. Our clinical experiments on five patients who underwent brain surgery with a navigation system show that optimizing one marker location and the anatomical landmarks configuration reduced the TRE. The average TRE values using the usual fiducials setup and using the suggested method were 4.7 mm and 3.2 mm, respectively. We observed a maximum improvement of 4 mm. Reducing the target registration error has the potential to support safer and more accurate minimally invasive neurosurgical procedures.**

***Index Terms*—Accuracy, image-guided neurosurgery, localization and tracking, rigid registration, therapy planning.**

I. Introduction

IMAGE-GUIDED surgery (IGS) has become the standard of care for many neurosurgical procedures. A key step in IGS is accurate intraoperative alignment, known as rigid registration, between preoperative MRI/CT images and the intraoperative physical anatomy. Rigid registration consists of finding the rigid transformation—described by three position and three orientation parameters—that achieves the best match between corresponding preoperative and intraoperative features of interest. A point-based registration method is often used in existing IGS systems [1]–[5]. It calls for localizing several (5–10) predefined points, usually referred to as fiducial points, on the preoperative MRI/CT images, and correlating them with their counterparts on the intraoperative physical anatomy. Fiducial points can be implanted spheres, bone screws, adhesive skin markers, and anatomical landmarks. In the following paper, we are using the term "fiducial markers" for adhesive skin markers and bone mounted markers.

Quantifying the registration error is of great clinical importance, as it has direct implications for treatment decisions and assessment of the risk of a specific intervention. The most clinically relevant measure is the target registration error (TRE), which is the distance between the target location defined on the preoperative image and the corresponding target location on the physical head after intraoperative registration. For example, in image-guided brain biopsy, the intracranial target biopsy location is reached by following the location of the biopsy needle tip in preoperative images. If the actual tip location is too far from the desired target location, the biopsy diagnosis may fail and undesired complications may occur. The clinically relevant error measure is thus the actual final location of the needle tip with respect to the image-defined target, rather than a different commonly used measure, the fiducial registration error (FRE). The FRE is defined as the root mean square (RMS) distance between the location of fiducial points on images and their physical location, after registration [6]. Clinical observations show that the correlation between the FRE and TRE is often weak, with large deviations between these two measurements [7]–[10]. Moreover, it was also recently shown that the FRE and TRE are statistically uncorrelated in a variety of realistic situations [11]–[14].

A. TRE Estimation

Since targets are usually inside the anatomy, TRE cannot be directly measured; it has to be estimated from other available measurements [6]. The TRE is directly related to the Fiducial localization error (FLE), which is the discrepancy between the selected and the actual (unknown) fiducial point locations. Estimation of the TRE plays a central role in determining the expected surgical localization error and in evaluating the potential risk the outcome of a surgery. As a result, TRE estimation has been the subject of much research [6], [12], [15]–[22]. Table I summarizes the characteristics of various TRE estimation techniques. These are analytical techniques that require a model of FLE distribution and a registration method. FLE distributions can be: 1) isotropic/anisotropic, depending on whether FLE magnitude is the same in all directions (isotropic) or not (anisotropic); 2) homogeneous/heterogeneous, depending on whether the distribution of FLE is the same for all fiducial points (homogeneous) or not (heterogeneous), and; 3)

Manuscript received June 24, 2011; revised November 02, 2011; accepted November 07, 2011. Date of publication December 06, 2011; date of current version March 02, 2012. This work was supported by the FP7 ERC ROBOCAST Grant 21590. *Asterisk indicates corresponding author.*

*R. R. Shamir was with the Rachel and Selim Benin School of Engineering and Computer Science, The Hebrew University of Jerusalem, 91904 Jerusalem, Israel. He is now with the Edmond and Lily Safra Center for Brain Sciences, Medical Neurobiology and Neurosurgery Departments, The Hebrew University and Hadassah Medical Center, 91120 Jerusalem, Israel (e-mail: shamir.ruby@gmail.com).

L. Joskowicz is with the Rachel and Selim Benin School of Engineering and Computer Science, and with the Edmond and Lily Safra Center For Brain Sciences, The Hebrew University of Jerusalem, Jerusalem 91904, Israel (e-mail: josko@cs.huji.ac.il).

Y. Shoshan is with the Neurosurgery Department, Hadassah Medical Center, and with the Faculty of Medicine at the Hebrew University of Jerusalem, 91120 Jerusalem, Israel (e-mail: yigalshoshan@mac.com).

Digital Object Identifier 10.1109/TMI.2011.2175939

TABLE I
ESTIMATION METHODS FOR TARGET REGISTRATION ERROR

TRE estimation method	Isotropic/ anisotropic FLE distribution	Homogeneous/ heterogeneous FLE distribution	Biased/ unbiased FLE distribution	Registration method
1. Fitzpatrick et al. [6]	*isotropic*	*homogeneous*	*unbiased*	*least squares*
2. Wiles et al. [18]	*anisotropic*	*homogeneous*	*unbiased*	*least squares*
3. Danilchenko et al. [12]	*anisotropic*	*heterogeneous*	*unbiased*	*weighted least squares*
4. Moghari et al. [17], Ma et al.[16]	*anisotropic*	*heterogeneous*	*unbiased*	*maximum likelihood*
5. Moghari et al. [15]	*anisotropic*	*heterogeneous*	*biased*	*maximum likelihood*

Comparison of five analytic TRE estimation methods (first column) as a function of FLE distribution and registration method (first row).

unbiased/biased, depending on whether the expected value of the FLE distribution is zero (unbiased) or not (biased). The most common registration methods minimize the RMS distance of the fiducials (least-square methods). Others, assign weights to the fiducial points (weighted least squares), use maximum likelihood methods, and/or incorporate more realistic FLE models.

We determined in a recent study that actual FLE in a clinical neuronavigation setup is anisotropic and heterogeneous in both magnitude and direction; i.e., for each fiducial point, FLE is anisotropic with respect to different principal axes [8], [23]. When surgical tool calibration errors, inflammatory effects of sedation, potential human errors in the manual fiducial points selection and pairing process are taken into consideration, it is most likely that the FLEs also include a bias and interdependencies with each other [8], [23], [24]. Existing analytical TRE estimation methods do not account for dependencies between fiducial points FLEs, despite the apparent advantage of taking this factor into consideration. Moreover, analytical methods do not always provide a convenient way for computing the percentile value (e.g., 95%), which provides a TRE confidence level that is useful in assessments of neurosurgical risks.

B. Fiducial Marker Optimization

The placement of the adhesive or implanted fiducial markers and the selection of the anatomical landmarks have a direct influence on actual TRE [9], [25]–[29]. Since the actual TRE is unknown at the registration phase, methods for TRE estimation can be used to optimize fiducial locations and to analyze their effect on the TRE. West *et al.* [9] propose three guidelines for good fiducial points placement: 1) use as many fiducial points as possible; 2) ensure that the fiducial points center of mass is as close as possible to the target location; and 3) avoid nearly collinear fiducial points locations. While simple, these guidelines are not always intuitive and easy for surgeons to follow, especially when multiple targets are considered. Moreover, it has been recently shown [8], [11], [13] that following these guidelines may not always reduce the TRE.

Liu *et al.* [29] describe a genetic algorithm that approximates optimal fiducial points placement by minimizing the TRE estimated using the method of Fitzpatrick *et al.* [6]. The algorithm was evaluated on abdominal and thoracic phantoms with a photogrammetric positioning system. The study shows that optimizing a set of randomly placed fiducial points reduced the average TRE from 1.9 mm to 0.8 mm. Riboldi *et al.* [28] combine genetic and taboo search to minimize the estimated TRE. Their simulation study on 10 datasets of prostate patients shows that optimizing a set of randomly placed fiducial points with their method reduces the TRE by 26% versus 19% with a genetic algorithm. Atuegwu *et al.* [27] incorporate a skin motion model and approximate optimal landmark placement for a target region based on the TRE estimation. Their phantom and simulation studies show a mean TRE improvement of 1.5 mm. Wang *et al.* [25] describe an interactive method for the optimization of the fiducial point locations that incorporates TRE estimation, and presents a mean accuracy improvement of 0.5 mm. Note that all these works use the TRE estimation method described in Fitzpatrick *et al.* [6].

To summarize, existing studies and solutions suffer from one or more of the following limitations: 1) the methods were tested on a phantom or with a simulation on MRI/CT images, and thus do not measure the actual intraoperative TRE; 2) most methods depend on an ad-hoc initialization and are thus only locally optimal; 3) all methods use the analytic TRE estimation method by Fitzpatrick *et al.* [6], which is not always a good estimation of the actual TRE [8], [23]; 4) no quantitative feedback, user interaction, or error visualization is provided to help the user override system selection of fiducial points based on patient-specific anatomical and surgical criteria (except to a limited extent for Wang *et al.* [25]); and 5) no previous study has quantified the actual improvement in accuracy that can be achieved by optimizing both adhesive markers placement and anatomical landmarks selection.

In this paper, we present three new methods to improve localization accuracy in keyhole image-guided neurosurgery by optimizing the use of fiducial points for computing the image-to-patient registration. The first method finds the anatomical landmarks and fiducial markers (e.g., skin adhesive or bone mounted markers) subset that yields the smallest TRE. The second method finds the set of optimal fiducial markers placements that yield the smallest TRE. The third method supports interactive fiducial markers placement with an interactive visualization and evaluation software module that provides quantitative feedback to neurosurgeons that allows them to override system selection and explore alternatives. In all cases, the optimization is based on empirically derived FLE models and simulation-based TRE estimation. To validate our approach, we compare our simulation-based TRE estimation method with two analytical methods and evaluate their effectiveness for fiducial points optimization. We show how these methods can be incorporated into the standard neurosurgical IGS workflow with no additional imaging and with minor modifications, and validate them and the protocol in a clinical setup on five patients.

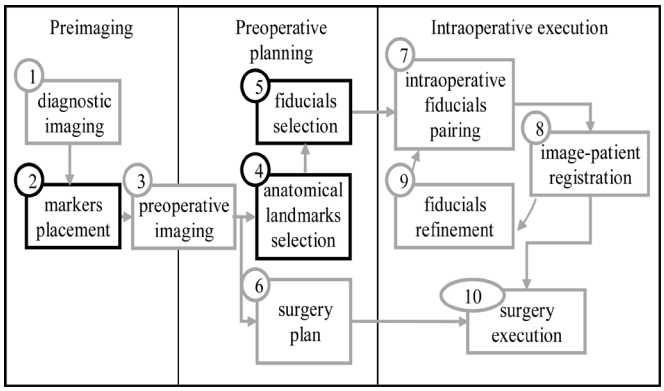

Fig. 1. Protocol for accuracy optimization of point-based registration in image-guided neurosurgery. Bold frames indicate the protocol steps we propose to improve with our methods.

This paper is organized as follows. In Section II, we describe the current IGS workflow and the role of fiducial marker placement and anatomical landmark selection, and show how to incorporate our methods into this workflow. In Section III, we present the point-based rigid registration problem and define the relevant error terms. In Section IV, we discuss FLE models and their effect on TRE. We go on to describe our simulation-based TRE estimation method, which is based on empirically-derived FLE models. In Section V, we describe three new methods for optimal selection of anatomical landmarks, for optimal fiducial marker placement, and for interactive fiducial marker placement based on interactive quantitative visualization. In Section VI, we present the clinical experiments and results. In Sections VII and VIII, we discuss the significance of our results and conclude with possible directions for future work.

II. Image-Guided Neurosurgery: Overview of Methods and Workflow

The routine IGS procedure for neurosurgery consists of three stages: diagnostic and preoperative imaging, preoperative planning, and intraoperative execution (Fig. 1). In the diagnostic and preoperative imaging stage, CT and/or MR scans of the patient are acquired (1. *diagnostic imaging*). These scans are usually acquired several weeks before surgery and are low-resolution, with 2–5 mm slice thickness. Once it is determined that keyhole neurosurgery is indicated, a few adhesive skin markers and/or skull bone screws are placed on the patient's head shortly before surgery (2. *fiducial marker placement*). New high-resolution CT/MRI scans are acquired, usually within a day of surgery (3. *preoperative imaging*).

In the preoperative planning stage, imaging studies are uploaded to the planning station, and fiducial marker locations and the outer head surface are automatically extracted. The neurosurgeon then defines the anatomical landmarks to be used for registration (4. *anatomical landmark selection*), combines them with the fiducial markers, and determines which fiducial points—including anatomical landmarks and fiducial markers—will be used for intraoperative registration (5. *fiducial selection*). The neurosurgeon then defines the entry and target points in the planning station (6. *surgery plan*) and saves the resulting preoperative data. In the intraoperative execution stage, the preoperative plan and CT/MRI studies are uploaded into the operating room IGS station. Before the start of the surgery, the surgeon touches the fiducial markers and anatomical landmarks with a navigation pointer, thereby pairing them for registration (7. *intraoperative fiducial pairing*). Once the image-to-patient registration is performed (8. *image-to-patient registration*), the surgeon evaluates system localization accuracy. If not satisfied, the surgeon adds and/or deletes fiducial points in an attempt to improve localization accuracy (9. *fiducial refinement*). Once the surgeon is satisfied, IGS proceeds and surgery is performed according to plan (10. *surgery execution*).

The current IGS workflow does not guarantee the best achievable localization accuracy for the following key reasons.

1) Prior to preoperative imaging, the fiducial markers are placed on the patient's head by the imaging technician, based on previous experience, aesthetic considerations, and/or personal preference. Therefore, their location may not be optimal.
2) During preoperative planning, the surgeon selects the anatomical landmarks and fiducial markers that will be used for intraoperative registration without knowing what the expected TRE will be.
3) In the operating room, registration is performed based on the preselected fiducial points. This selection might not minimize the actual TRE, especially when one or more fiducial points are no longer available, e.g., a fallen adhesive marker or an anatomical landmark that becomes inaccessible when the patient is draped for surgery.
4) When the reported accuracy is not satisfactory, the surgeon adds and/or removes fiducial points manually to try to improve accuracy. This process is time consuming and does not guarantee the best possible result [1], [11], [15].

We propose to overcome these limitations with an approach that guarantees the lowest possible estimated TRE with no additional imaging and only minor modifications to the IGS workflow. Our approach introduces improvements at three primary IGS workflow stages.

The first improvement is to compute suggested optimal fiducial marker locations using the routine diagnostic scan. Prior to preoperative imaging, before placing the fiducial markers on the patient's head, the early lower-resolution diagnostic images are loaded into the preoperative planning station. Following automatic extraction of the outer head surface, the neurosurgeon defines one or more target points on the scan slices, and one or more entry points and anatomical landmarks on the outer head surface. Then, our method computes the set of optimal fiducial marker placements that minimize the estimated TRE value based on empirical precomputed image and physical FLE models. The surgeon can then interactively add or modify fiducial marker placement on the outer head surface with feedback regarding the estimated TRE.

Each point on the surface represents an option for fiducial marker placement. To facilitate the surgeon's decision making process, we compute and present a map that is color-coded to reflect the magnitude of estimated TRE with fiducial marker placement on different areas of the head surface (Fig. 2). Computations take into consideration the predefined target location and the effects of previously selected anatomical landmarks and

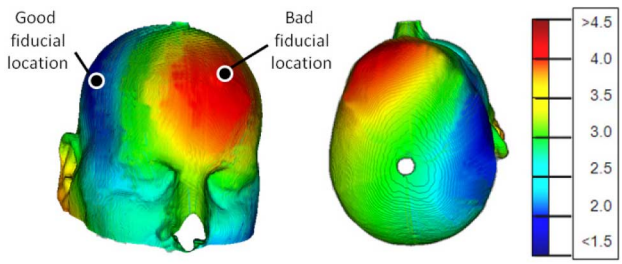

Fig. 2. Estimated color TRE map showing the expected error obtained by adding fiducial markers at two locations on the patient head surface. "Good" fiducial marker locations with small TREs and "bad" locations with large expected TREs are shown. The expected TRE values (in mm) are color-coded as shown on the scale to the right.

fiducial markers. Considering that the fiducial markers cannot be placed precisely at planned locations, the user can select a fiducial marker placement in the middle of a zone that is associated with a low estimated TRE, such that even if the fiducial marker is placed with some deviation from the planned location, the impact on the estimated TRE will remain low. The TRE map is also useful for choosing an extra fiducial marker, should one of the selected markers fall off. An extra fiducial marker can be placed in a zone on the head surface with low estimated TRE values, indicating a good alternative fiducial marker location.

This TRE map is computed based on diagnostic images obtained several weeks or even months before surgery. Once satisfied that the TRE is acceptable for the planned procedure, the surgeon or the imaging technician places fiducial markers on the patient's head according to the map and preoperative scans are acquired. The anatomical landmarks and fiducial markers subset that minimize the TRE may be different at the date of the surgery because of changes in image quality, errors in fiducial marker placement, and intracranial morphological changes that may affect the target location and thus optimal fiducial points.

The second improvement is a new computation of the optimal subset of anatomical landmarks and fiducial markers based on the higher quality preoperative images and final selection of the target location. Our method automatically computes the optimal anatomical landmark and fiducial marker subset that yields the lowest TRE based on the estimated FLE models and TRE. This simplifies the fiducial refinement step and provides the surgeon with a preoperative measure of what is expected in the operating room.

The third improvement is the computation of the optimal anatomical landmark and fiducial marker subset in the operating room. Following acquisition of actual anatomical landmark and fiducial marker locations with the tracked probe, we compute the optimal landmarks and fiducial markers subset that yields the lowest TRE considering both preoperative and intraoperative localization data. This simplifies the fiducial refinement step working with actual values at surgery. While additional time is required before the preoperative imaging, it saves time in preoperative planning and intraoperative execution by taking out the guesswork of fiducial points selection, and can greatly increase the accuracy.

III. Point-Based Rigid Registration

Here, we formally describe problems associated with point-based rigid registration, and introduce registration error terminology. We use the following conventions for the mathematical notation: Greek letters denote scalars and/or common abbreviations used in the literature; Roman lowercase letters denote points; Roman lowercase letters with arrows above them denote vectors; Roman capital letters denote groups and matrices.

Let $A = \{a_1, a_2, \ldots, a_n\}$ and $B = \{b_1, b_2, \ldots, b_n\}$ be two sets of n paired points, each in its own coordinate system. Each point represents a fiducial point, which can be an implanted sphere, a screw skull marker, an adhesive skin marker, or an anatomical landmark. Since the fiducial points locations are determined from images (automatically, or manually on a computer screen), or from a localization device in physical space, their location is subject to inaccuracies and measurement errors.

Fiducial Localization Error (FLE) is the vector between the measured and the unknown actual fiducial points locations. The FLE vector size is called **FLE magnitude**. We define the sets of measured fiducial points locations as

$$P(A, L_A) = \{p_i | p_i = a_i + \overrightarrow{l_{a_i}}\}_i$$
$$Q(B, L_B) = \{q_i | q_i = b_i + \overrightarrow{l_{b_i}}\}_i \quad (1)$$

where a_i and b_i are the exact fiducial points locations, and $\overrightarrow{l_{a_i}}$ and $\overrightarrow{l_{b_i}}$ are their FLE vectors, respectively. L_A and L_B are the sets of FLE vectors. Note that this definition allows modeling many localization error functions, and can incorporate both deterministic and random components. In the following sections we use the shorthand notations P and Q to denote $P(A, L_A)$ and $Q(B, L_B)$, respectively.

Let T_P^Q be the rigid transformation—rotation and translation—that minimizes the RMS distance between corresponding fiducial points pairs $\{(p_i, q_i)\}_i$. This transformation is computed to align coordinate systems A and B. The sets P and Q correspond to the sets A and B with fiducial points localization errors. We assume throughout the paper that P and Q have at least three noncollinear fiducial points.[1]

Let $\overrightarrow{\mathrm{FRE}}_i$ be the **FRE vector** of pair (p_i, q_i), defined as the vector between fiducial points locations after registration, $\overrightarrow{\mathrm{FRE}}_i = T_P^Q p_i - q_i$. The **FRE** of fiducial points pair i, denoted by FRE_i, is the norm $\mathrm{FRE}_i = |\overrightarrow{\mathrm{FRE}}_i|$. The FRE of fiducial points sets P and Q is

$$\mathrm{FRE}(P, Q, T_P^Q) = \sqrt{\frac{\sum_{i=1}^{n} \mathrm{FRE}_i^2}{n}}. \quad (2)$$

For consistency with the literature, the FRE is defined as the RMS of the FRE vector magnitudes. Note that other statistics of the FRE vectors such as mean, variance, and 95th percentile can also be computed; however, we do not consider them further, as they are not required in this paper.

[1]Recently, new methods for computing the registration parameters with more realistic FLE models have been suggested [30], [31]. We do not employ them in our study since they are not yet widely used and are most likely not incorporated in commercial navigation systems under consideration here.

Let a_{target} be a target point in coordinate system A, and b_{target} the corresponding point in coordinate system B. Without loss of generality, we assume that target location a_{target} is known, and that its corresponding location b_{target} is unknown.

Since b_{target} is usually inside the anatomy, it cannot be measured, and thus q_{target} is not available. For simplicity and clarity, we restrict our discussion in the following sections to a single target location; the generalization to multiple targets is readily made.

Let $\overrightarrow{\text{TRE}}_{\text{target}}$ be the **TRE vector** of pair $(a_{\text{target}}, b_{\text{target}})$, defined as the vector between the target location after registration, $\overrightarrow{\text{TRE}}_{\text{target}} = T_P^Q a_{\text{target}} - b_{\text{target}}$. Note that the transformation T_P^Q is computed using the measured fiducial points locations P and Q, but the TRE is computed with respect to the actual target location b_{target}. In practice, the transformation is computed from measured fiducial points, although from a clinical perspective, it is the true target location discrepancies that are of interest.

The norm $|\overrightarrow{\text{TRE}}_{\text{target}}|$ is the **TRE**, defined as

$$\text{TRE}\left(a_{\text{target}}, b_{\text{target}}, T_P^Q\right) = |\overrightarrow{\text{TRE}}_{\text{target}}|. \tag{3}$$

For consistency with the literature, we refer to **FRE** and **TRE** as scalar error values. The **FRE vector** and **TRE vector** refer to their respective directional errors. To distinguish between the **FLE** vector and its magnitude, we explicitly use the term **FLE magnitude** to indicate FLE vector size. Vector error parameters are denoted with an arrow above the relevant term.

IV. Simulation-Based TRE Estimation Incorporating Empirical FLE Models

We propose to use an empirical, simulation-based TRE estimation method that is based on actual measurements. We model the FLE as biased, isotropic, independent, and with an inhomogeneous normal distribution. The direction of the FLE was drawn randomly on the unit sphere from a uniform distribution. The FLE magnitude distribution of a fiducial point a_i is one-dimensional and normally distributed with a bias $|l_{a_i}| \sim N(\mu_{a_i}\sigma_{a_i})$. The Standard Deviation (SD), σa_i, is estimated by computing the SD of distances between repetitive selections of the same fiducial point.

Recent studies indicate the possible presence of a bias in the FLE [8], [15]. Likely sources for this bias include user manipulation errors, swelling due to patient sedation, unstable patient fixation, MRI image distortion and limited resolution, suboptimal registration of fiducial marker configuration, tracked tool calibration error, and human error in the identification and pairing of anatomical landmarks, among others [8], [11], [24], [32], [33]. What constitutes a good model for this bias remains an open question and is beyond the scope of this paper.

For our study, we choose the average of distances between repetitive selections of the same fiducial point to model FLE bias μ_{a_i}. The FLE of fiducial points set A, denoted as L_A, is the set of its individual fiducial points FLEs, $L_A = (\overrightarrow{l_{a_1}}, \overrightarrow{l_{a_2}}, \ldots, \overrightarrow{l_{a_n}})$. The FLEs of fiducial points set B are defined similarly and denoted as L_B.

We chose an isotropic model because, at the time of our experiment, the actual average FLE magnitude was the only information available from the neuronavigation system. The anisotropic analysis was only performed later on data that we gathered. Modeling of an anisotropic FLE distribution based on this clinical data requires more data and further investigation, considering the varying FLE principal axes (see Section VI-1). Wiles and Peters propose to estimate the FLE parameters online from the FRE [34]. However, we have shown that the FRE can be greatly affected by some FLEs and remain nearly invariant for others [11]. As the FRE-FLE relation in our setup is unknown, we chose to avoid FLE estimation from FRE values.

Table II shows the proposed TRE estimation method. The inputs are a set of fiducial points and one or more targets defined on the preoperative CT/MRI images, the mean and standard deviation from prior FLE models computed from previous surgical localization data, and the number of samples, M, on which the estimation will be based. In the first step, simulated image and physical FLEs are randomly generated based on the prior FLE models. The simulated FLE values are added to the fiducial points locations to obtain fiducial points location perturbations (step 2). The rigid transformation between the two perturbed fiducial points sets is computed to model the effect of the FLE on the TRE (step 3). The target locations are then perturbed according to their recorded localization errors (step 4), prior to applying registration transformation on the target locations. This simulates TLE that is due to sources other than FLE, such as the navigation system, imaging modality, and user errors. Finally, the computed transformation is applied on the perturbed target locations, and the TRE is estimated (step 5). This process is repeated M times, and average of estimated TREs is computed. Additional statistical TRE estimation values, such as the standard deviation or 95% TRE percentile are computed as needed.

The simulation-based TRE estimation method has the following potential advantages. 1) Any FLE distribution can be used, including those with heterogonous principal axes directions. 2) No FLE distribution model is necessary. When the FLE sample dataset is sufficiently large, FLE values can be drawn by randomly selecting an FLE from the recorded dataset. 3) The simulation yields a histogram characterizing the TRE distribution, and thus allows direct access to the xth percentile. 4) The TRE direction is also provided, not only its RMS value. Its disadvantages are that it is computationally more expensive than analytical methods and may be more sensitive to FLE data errors, which are not modeled.

V. Fiducial Marker Placement and Anatomical Landmark Selection

We now describe three localization accuracy optimization methods: 1) fiducial points subset selection; 2) preimaging fiducial marker placement; and 3) interactive fiducial markers placement.

A. Fiducial Points Subset Selection

Fiducial points selection is the task of selecting from a given initial set of fiducial points, the subset that minimizes the esti-

TABLE II
SIMULATION-BASED TRE ESTIMATION METHOD

Input: A - a set of n fiducials on the image
a_{target}- target location on the image
$\left\{\mu_{a_i}, \sigma_{a_i}\right\}_{i=1}^{n}$ and $\left\{\mu_{b_i}, \sigma_{b_i}\right\}_{i=1}^{n}$ - FLE distribution parameters
M - number of desired samples

EstimateTRE(A, a_{target}, $\left\{\mu_{a_i}, \sigma_{a_i}\right\}_{i=1}^{n}, \left\{\mu_{b_i}, \sigma_{b_i}\right\}_{i=1}^{n}$ ***)***

Repeat the following steps $m=1,2,..,M$ times

1) Draw random values for L_A and L_B from
$$\left\{\mu_{a_i}, \sigma_{a_i}\right\}_{i=1}^{n} \text{ and } \left\{\mu_{b_i}, \sigma_{b_i}\right\}_{i=1}^{n}$$
2) Perturb fiducials locations:
$$p_i = a_i + l_{a_i},\ q_i = a_i + l_{b_i},$$
$$P = \left\{p_i\right\}_{i=1}^{n} \text{ and } Q = \left\{q_i\right\}_{i=1}^{n}$$
3) Compute T_P^Q, the rigid registration transformation between the perturbed fiducials.
4) Perturb targets locations.
$$p_{target} = a_{target} + l_{a_{target}},\ q_{target} = a_{target} + l_{b_{target}}$$
5) Compute the TRE occurred by this perturbation.
$$ETRE_m = \left| T_P^Q \cdot p_{target} - q_{target} \right|$$

Output: $\sum ETRE_m / M$, the average estimated TRE.

The input is a set of fiducials and a target defined on the clinical preoperative image, and statistical parameter values. The output is the estimated mean TRE.

mated TRE. Let A and B be two sets of preoperative and intraoperative fiducial points, and a_{target} the target location. The goal is to find the optimal fiducial points subset pairing that minimizes the estimated TRE (ETRE)

$$(A^*, B^*) = \underset{\substack{A' \subseteq A \\ B' \subseteq B}}{\arg\min}\, \text{ETRE}(a_{\text{target}}, A', B', \text{FLE}) \quad (4)$$

where FLE is the FLE model parameters, and the ETRE refers to the TRE estimation method. The method may incorporate image-based and/or physical fiducial points locations. For image fiducial points only, the method is useful for selection of the best anatomical landmark subset in the preoperative stage. For physical fiducial points, the method is useful to refine the selection of anatomical landmarks and adhesive fiducial markers in the operating room before registration.

The most direct method of finding the optimal pairing and transformation is to enumerate all possible pairings $A' \subseteq A$ and $B' \subseteq B$, compute the ETRE for each pairing, and select the subset of pairings that yield the smallest value. This exhaustive enumeration is feasible when both A and B are small, or when the total number of fiducial pairings can be restricted. This is, in fact, the case in current commercial systems, which limit the number of fiducial points pairs to a dozen. In this case, the total number of pairings is never greater than $2^{12} = 4\,096$, enabling computation of all possible ETREs on a standard PC in a few seconds.

B. Fiducial Marker Placement

Fiducial marker (e.g., skin adhesive or bone mounted marker) placement is the task of defining locations and placing fiducial markers on the patient's head before preoperative imaging. Let A be a set of preoperative fiducial points (e.g., fiducial markers and anatomical landmarks) and a_{target} the target location. The goal is to find the locations of one or more fiducial markers such that the joint set of fiducials $A^{\#}$ minimizes the ETRE

$$A^{\#} = \underset{A' \subseteq S}{\arg\min}\, \text{ETRE}(a_{\text{target}}, A \cup A', \text{FLE}) \quad (5)$$

where A' is selected from a set of points on the anatomy surface S (in image coordinates).

A direct method to find the optimal set of fiducial marker locations is as follows. First, we evenly sample points on the head surface, S, extracted from the MRI/CT to obtain a set of potential fiducial marker locations, P. Then, we compute the ETRE value for each possible small subset (e.g., 3–12 points) of P, and select the one with the minimum ETRE value. The exhaustive search approach requires $\binom{|P|}{k}$ candidate fiducial markers locations for k markers, where $|P|$ stands for the size of set P. A typical head surface reconstruction contains tens of thousands of points, therefore, searching the optimal configuration for four fiducial markers over a 10 000 points data set, results in over 4×10^{14} different configurations! Previous studies [9], [25], [27]–[29] suggest starting with a random fiducial marker configuration and then iteratively refining the fiducial marker locations until a minimum is achieved. This is repeated for additional random configurations until the minimal TRE is found. The main drawbacks of these methods are that: 1) the result depends on the initial fiducial marker configuration; 2) the optimization is local; and 3) the number of fiducial markers is predetermined.

We propose the following alternative approach. Since ETRE values are locally continuous and have small variability for small fiducial marker location changes (Section VI), we select a small set of uniformly distributed representative points on the surface S and then perform an exhaustive search as described above on each set. First, we compute the optimal landmark set $A^{\#}$ on a small set of potential fiducial marker locations, P, sparsely sampled on S. Then, for each fiducial marker in $A^{\#}$, we define a neighborhood on S and build a quad-tree hierarchical spatial data structure rooted at the selected fiducial marker. For each fiducial marker, we find its four descendants on the quad-tree, compute the ETRE of all possible combinations, and select the one with the smallest ETRE.

C. Interactive Fiducial Markers Placement Based on Risk Visualization

For practical and clinical reasons, the surgeon may need to modify the optimal computed fiducial markers configuration. For this purpose, we have developed a method that allows the surgeon to add and/or remove the selected fiducial markers and anatomical landmarks with visual error feedback, where the estimated TRE values are color-coded and superimposed on the patient head surface that was extracted from the MRI image (Fig. 2).

Given the target and selected fiducial markers locations, colors on the resulting TRE map show the predicted TRE after the addition or location change of a fiducial marker. If the neurosurgeon is interested in adding a fiducial marker, then the method colors the surface taking into consideration preselected anatomical landmarks and fiducial markers. When a fiducial marker is relocated, the method deletes the fiducial marker from the fiducial points sets and recolors the head surface accordingly. The coloring convention is as follows: blue zones are associated with high accuracy and low predicted TRE values; red zones are associated with poor accuracy and high predicted TRE values. Therefore, adding a fiducial marker on a blue zone is expected to improve targeting accuracy. The method also allows the neurosurgeon to incorporate clinical information into fiducial planning and to avoid anatomical landmarks that are difficult to locate or that are located at areas known for large skin deformations. Although this does not guarantee optimality, it keeps the surgeon in control and allows the incorporation of additional personal and experience-based considerations.

VI. Experimental Results

To validate our methods, we conducted three experiments: 1) empirical derivation of the FLE model; 2) evaluation of the TRE estimation method for optimal fiducial placement and selection, and; 3) assessment of the effect of optimal fiducial selection and placement methods on the actual TRE.

A. Empirical Derivation of the FLE Distribution

Experiment: We characterize the FLE bias and variance (see Section 4) from localization data that was gathered in a clinical experiment on 12 patients who underwent brain biopsy with a standard navigation system [8], [23]. Preoperatively, the neurosurgeon defined 7–12 different fiducial points (anatomical landmarks and adhesive fiducial markers) on the patient's MR image. Each MR image consists of $512 \times 512 \times 160$ voxels, with a voxel size of $0.47 \times 0.47 \times 1.0$ mm^3. Intraoperatively, the surgeon touched the physical fiducial points with a tracked pointer and correlated them with their corresponding locations on the MRI images. The pointer location was recorded directly from the StealthStation navigation system (Medtronic Inc., Minneapolis, MN). Each landmark was repeatedly selected 3–6 times on both the preoperative image and intraoperative physical anatomy. In the laboratory, we computed fiducial points FLE as described above from repetitive selections of each fiducial for all patients on both the MRI image and the physical space.

We then combined the localization error data of all patients such that each fiducial is associated with a set of FLE vectors on the MRI image and a set of FLE vectors on the physical space. Next, we computed the principal axes of the resulting FLE vectors using singular value decomposition (SVD) as described below. Following the automatic reconstruction of the head surface, we computed the rigid transformation between the physical space and the surface coordinate system, and applied it to the physical FLE data to align both datasets to the surface coordinate system. We then superimposed the principal FLE axes of all fiducial points for both the MRI image and the physical space on the head surface, to visualize the correlation between the FLEs and the geometric features of the patient's head. For the image-to-physical space registration, we used Horn's closed-form analytical least-squares method, both because it is the most popular registration method and because it is the method used in commercial navigation systems, allowing us to test our method in a clinical environment.

The principal axes of the resulting FLE vectors were computed as follows. Given a set of mean-centered k FLE vectors in a matrix form M of size $3 \times k$, we compute its SVD decomposition, $M = U\Sigma V$, where U is a 3×3 unitary matrix, Σ is a $3\times$k diagonal matrix with the singular values of M on its diagonal, and V is a $k \times k$ unitary matrix. Assuming that the set of FLE vectors contain at least three non-coplanar vectors, each column of U is defined as a principle axis vector with respect to the given set of FLE vectors. The column in U that is associated with highest singular value is associated with highest variability of FLE vectors, and the column that is associated with lowest singular value is associated with the lowest variability of FLE vectors.

Results: As reported in [8], the mean$\pm$SD of the fiducial localization errors for each fiducial type were as follows. 1) **left tragus**: MRI -0.6 mm ±0.5 mm, physical -1.9 mm ±1.0 mm; 2) **left helical cruz**: MRI -1.2 mm ±1.1 mm, physical -2.8 mm ±1.6 mm; 3) **left lateral cantus**: MRI -1.3 mm ±0.9 mm, physical -2.7 mm ±1.7 mm; 4) **left medial cantus**: MRI -1.1 mm ±0.9 mm, physical -2.1 mm ±1.3 mm; 5) **nose bridge**: MRI -1.2 mm ±1.0 mm, physical -1.9 mm ±1.1 mm; 6) **right tragus**: MRI -0.5 mm ±0.6 mm, physical -2.0 mm ±1.4 mm; 7) **right helical cruz**: MRI -2.0 mm ±2.0 mm, physical -3.0 mm ±1.6 mm; 8) **right lateral cantus**: MRI -0.9 mm ±0.7 mm, physical -2.3 mm ±1.4 mm; 9) **right medial cantus**: MRI -0.9 mm ±1.0 mm, physical -1.9 mm ±1.1 mm, and; 10) **marker**: MRI -0.8 mm ±0.6 mm, physical -1.6 mm ±0.9 mm.

Significant differences at the FLE magnitudes were observed among the anatomical landmarks and between the anatomical landmarks and adhesive skin fiducial markers. Also, the FLE on the MRI was dissimilar to that on the physical space. For example, the average FLE magnitude for localizing the adhesive skin fiducial markers on the physical space was 1.6 mm, compared to 3.0 mm and 0.5 mm for FLE magnitudes measured on the right helical cruz and right tragus, respectively. In this setup, the FRE and the TRE estimation computed with the method of Fitzpatrick *et al.* [6] are weakly correlated with the actual TRE, with discrepancies of up to 7 mm [8].

Fig. 3 shows the FLE variability at various fiducial points locations. For each fiducial point, the FLE magnitudes along the principle axes were different, and thus the FLE is anisotropic.

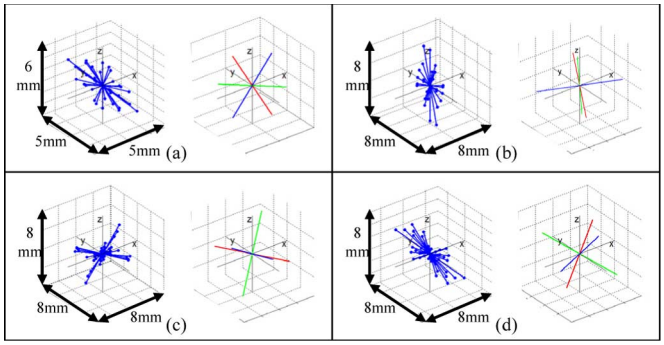

Fig. 3. FLE vectors for selected fiducial points as recorded *in vivo* with a navigation system (a)–(d), left). The FLE vectors' principle axes were computed for each fiducial point (a)–(d), right). The red axis is associated with the largest FLE variability, and the blue axis is associated with the lowest. FLE distribution is anisotropic and heterogeneous with varying principle axes. The selected fiducials are adhesive markers attached (a) above the right anterior part of the parietal bone; (b) above the left posterior part of the parietal bone and above the left part of the occipital bone; (c) at the right lateral cantus; and (d) at the right tragus.

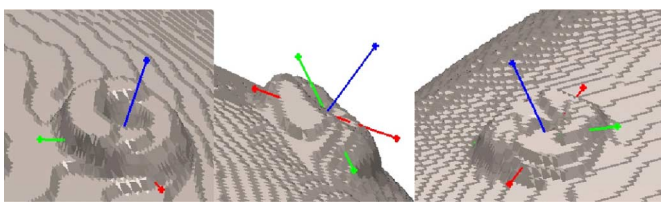

Fig. 4. Three examples of fiducial marker principal axes FLEs, as measured *in vivo* with a commercial navigation system on the outer surface of a patient's head. Note that the principal axes that are correlated with large FLEs (red and green axes) reside near the plan that is tangent to the head's surface.

For example, the tragus anatomical landmark, located near the ear, has 1.3 mm average FLE magnitude along one of its principal axes and 0.86 mm and 0.76 mm along the others. The overall FLE magnitudes also varied among the various fiducial points. Moreover, angular deviations of up to 90° were measured between the principal FLE axes that were associated with the lowest singular values.

We conclude from this study that clinical FLEs are heterogeneous and anisotropic with varying principal axes directions. Note that even the adhesive fiducial markers, which have comparable FLE magnitudes, can have very different principal axes. Another interesting result is that the FLE of adhesive fiducial markers on the physical space were found to have larger errors along the plane tangent to the head surface than along the axis that is perpendicular to the surface (Fig. 4).

B. Evaluation of the TRE Estimation Method

Experiment: To evaluate our simulation-based TRE estimation method with respect to the task of optimal fiducial points selection and placement, we added the following steps to the above protocol for each of the last five patients. Before preoperative imaging, the surgeon defined nine anatomical landmarks on the diagnostic image and one target location on the head skin. Then, the head surface was automatically reconstructed [36] and modeled with a set of points, each representing a possible fiducial marker location. For each point on the outer head surface, the TRE at the predefined target location was estimated

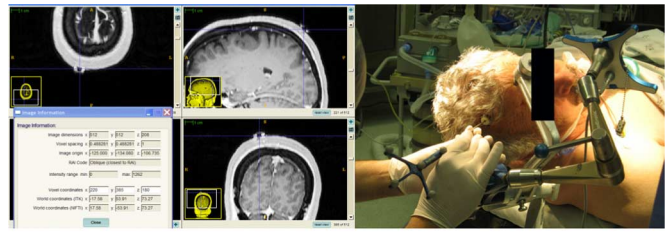

Fig. 5. Illustration of anatomical landmark and adhesive skin marker selection: (a) preoperatively, on the MRI image and (b) intraoperatively, on the patient's head with a commercial tracking system.

taking into account the anatomical landmarks with the method described in Section IV.

The TRE map was generated by mapping and color-coding the estimated TRE values on the outer head surface (Fig. 2).

Prior to preoperative imaging, three adhesive fiducial markers were affixed to the patient's head to approximate the good, bad and target locations. After MRI imaging with the standard navigation protocol, the surgeon localized the corresponding anatomical landmarks and the three fiducial markers on the patient's preoperative image [Fig. 5(a)]. In the operating room, two surgeons correlated the predefined fiducials as described in Section V-1 [Fig. 5(b)].

In the laboratory, the actual TRE values were computed as the distance between the image and physical measured target locations after registration. The actual TRE values were compared with TRE estimations computed with four different methods: 1) the analytical method of Fitzpatrick *et al.* [6], which assumes an unbiased, isotropic, and homogeneous FLE distribution; 2) the analytical method of Danilchenko *et al.* [12], which assumes unbiased, anisotropic and heterogeneous FLE distribution; 3) the homogeneous version of the simulation method (Table II) assuming a biased, isotropic, and homogeneous FLE distribution; and 4) the simulation method (Table II) assuming biased, isotropic and heterogeneous FLE distribution. For TRE estimation methods that assume heterogeneous FLE, the parameters $\{\mu_{a_i}, \sigma_{a_i}\}_{i=1}^{n}$ and $\{\mu_{b_i}, \sigma_{b_i}\}_{i=1}^{n}$ were computed from previous localization error data that was obtained in a similar setup (Section IV). For TRE estimation methods that assume homogeneous FLE distribution, we set the FLE parameters to be

$$\mu_a = \frac{\sum \mu_{a_i}}{n}, \quad \sigma_a = \frac{\sqrt{\sum \sigma_{a_i}^2}}{n}$$

and

$$\mu_b = \frac{\sum \mu_{b_i}}{n}, \quad \sigma_b = \frac{\sqrt{\sum \sigma_{b_i}^2}}{n}.$$

The analytical methods assume no bias, so μ was set to zero. For the evaluation of the TRE estimation methods, estimated TRE was compared to actual TRE for four fiducial configurations: 1) original predefined anatomical landmarks, and both good and bad fiducials; 2) original predefined anatomical landmarks and good fiducial placement; 3) original predefined anatomical landmarks and bad fiducial placement; and 4) original predefined anatomical landmarks. Overall, 180 different fiducial pairings

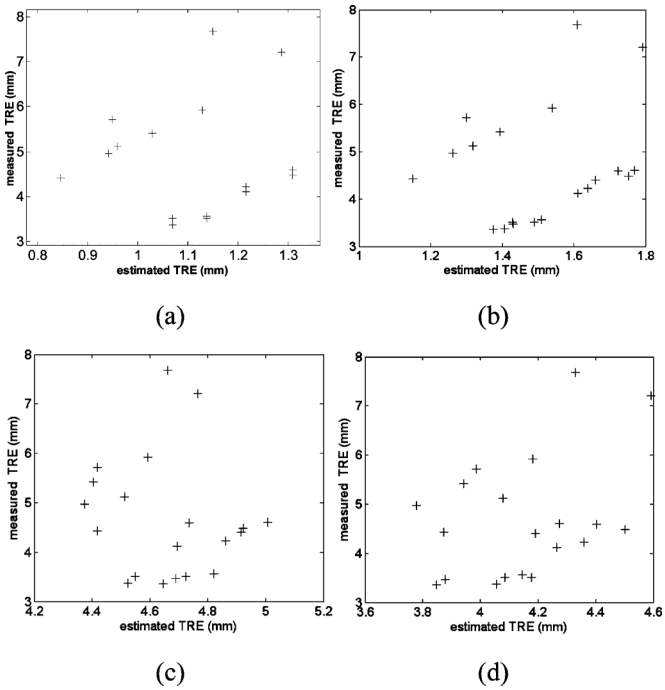

Fig. 6. Comparison of measured (average) and estimated TRE values. TRE was estimated using: (a) Fitzpatrick *et al.* [6]; (b) Danilchenko *et al.* [12]; (c) simulation with homogeneous FLE distribution, and; (d) simulation with heterogeneous FLE distribution. Then, the surgeon selected "good" and "bad" fiducial marker locations on the map. The good ones were associated with a low ETRE value and were expected to best improve accuracy; the bad ones were associated with a high ETRE value and were expected to yield less accurate targeting. In practice, we could not add more than three fiducial markers on the patient's head, so we could not test the multiple fiducial marker placement hierarchical optimization method.

were generated and analyzed from the four different fiducial configurations, the first three repetitive selections of the fiducial points on MRI images, the first three repetitive selections of same fiducial points on physical anatomy, and for five patients data $(4 \times 3 \times 3 \times 5 = 180)$.

Note that for the purpose of fiducials optimization, the TRE estimation does not have to accurately estimate the actual TRE; it only has to help decide if one configuration is better than another. That is, even if the estimated TRE is inaccurate, it can be useful for fiducial optimization as long as it is consistent. Therefore, we compared the differences in the actual and estimated TRE values and measured their correlation coefficients and p values. The null hypothesis was that the correlation between the values is zero; thus p values< 0.05 reject the null hypothesis and indicate that the correlation is higher than zero with a probability of at least 0.95. A total of 270 samples were measured from the six TRE differences (the number of pairs of configurations over the four defined above), the first three repetitive selections of the fiducial points on MRI images, the first three repetitive selections of same fiducial points on physical anatomy, and for five patients data $(6 \times 3 \times 3 \times 5 = 270)$.

Results: Fig. 6 compares the actual and estimated TRE for all patients and all TRE estimation methods. Table III summarizes the results. The average difference between the actual and estimated TRE and correlation coefficients were 0.9 ± 0.8 mm

TABLE III
EVALUATION OF TRE ESTIMATION METHODS

TRE DIFFERENCE	TRE ESTIMATION METHOD			
	Simulation heterogeneous	*Simulation homogeneous*	*Fitzpatrick et al. [6]*	*Danilchenko et al. [12]*
Mean (mm)	0.9	1.0	3.2	3.1
Std (mm)	0.8	0.7	1.5	1.2
Max (mm)	3.34	3.0	6.5	6.1
Correlation ρ	0.37	-0.13	0.17	0.22
p value	0.13	0.59	0.47	0.34

Summary of the differences between the actual and estimated TRE. The mean, standard deviation, and maximum differences between measured and estimated TRE as well as the correlation coefficient and the p value are shown for each of the four TRE estimation methods.

$(\max = 3.34$ mm), and $\rho = 0.37$ $(p = 0.13)$ using the simulation method with heterogeneous FLE distribution, 1.0 ± 0.7 mm $(\max = 3.0$ mm), $\rho = -0.13$ $(p = 0.59)$ using the simulation method with homogeneous FLE distribution, 3.1 ± 1.2 mm $(\max = 6.1$ mm), $\rho = 0.22$ $(p = 0.34)$ using the method of Danilchenko *et al.* [12], and 3.2 ± 1.5 mm $(\max = 6.5$ mm), $\rho = 0.17$ $(p = 0.47)$ using the method of Fitzpatrick *et al.* [6].

The results indicate no statistically significant correlation between the estimated and actual TREs. The simulation methods that incorporate a bias in the FLE model yield an estimated TRE value that was closer to the actual TRE in comparison to those of the analytic methods with unbiased FLE. Interestingly, in most cases the simulation and analytical methods with heterogeneous FLE did not yield a lower discrepancy between the actual and estimated TRE values with respect to the homogeneous simulation and analytical methods. However, the simulation and the method of Danilchenko *et al.* [12], with heterogeneous FLE distribution, did yield a higher correlation between the actual and the estimated TRE values, in comparison to methods with homogeneous distribution.

The general lack of improvement in differences between estimated and actual TRE with heterogeneous FLE can be explained by our previous paper [8], in which we argue that in certain circumstances a method can improve the expected TRE value, although for a specific selection of fiducial points, the discrepancies between actual and estimated TRE values may show no improvement. Note that for purposes of fiducial points setup optimization, the observed differences between the estimated and actual TREs do not invalidate the TRE estimation method.

Fig. 7 compares the actual and estimated TRE differences for all patients and all TRE estimation methods. The high relation between the values is readily observed. Fig. 8 shows a histogram of the p values for the correlation coefficients of differences in measured TRE values and differences in TRE estimated values for the analytical and simulation methods. For Fitzpatrick *et al.* [6], the average correlation coefficient is $\rho = 0.82$, and the average p value is $p = 0.08$. For Danilchenko *et al.* [12] $\rho = 0.91$, and $p = 0.02$. For our simulation method with a homogeneous FLE distribution, $\rho = 0.75$, and $p = 0.13$. Finally, for our simulation method with a heterogeneous FLE distribution, $\rho = 0.88$ and $p = 0.04$. We conclude that reducing the estimated TRE

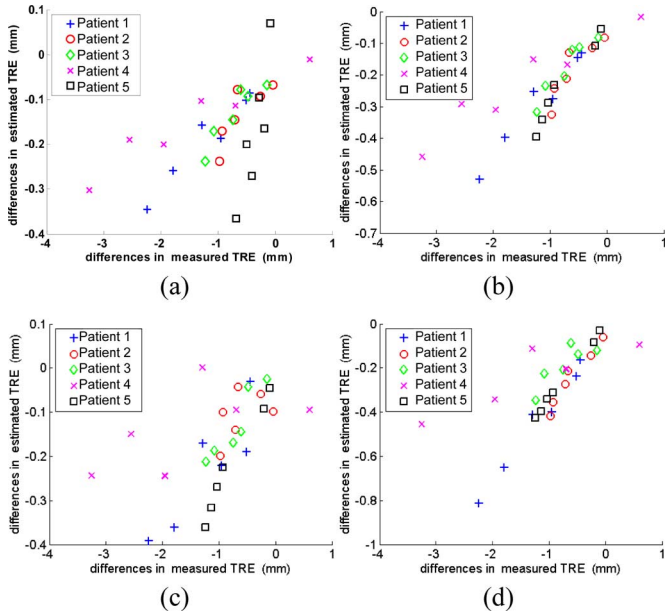

Fig. 7. A comparison of the actual (average) and estimated TRE differences reveals a strong relation between the values for all tested TRE estimation methods, namely: (a) Fitzpatrick *et al.* [6]; (b) Danilchenko *et al.* [12]; (c) simulation with homogeneous FLE distribution; and (d) simulation with heterogeneous FLE distribution. Therefore, all the methods are appropriate for deciding if one specific fiducial setup is better than another one, regardless of the differences between the actual and estimated TRE values.

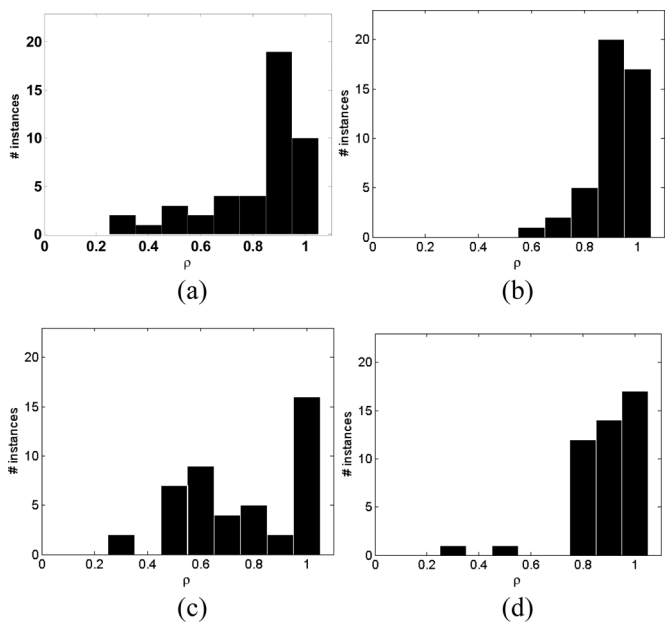

Fig. 8. FLE correlation histograms: ρ is the correlation coefficient value between estimated and measured TRE differences. The methods are: (a) Fitzpatrick *et al.* [6]; (b) Danilchenko *et al.* [12]; (c) simulation with homogeneous FLE distribution; and (d) simulation with heterogeneous FLE distribution.

will very likely reduce the actual TRE for both the analytical and simulation-based methods.

C. Effect of the Optimal Fiducials Selection and Placement Methods on the Actual TRE

Experiment: For the evaluation of the method for optimal fiducial marker placement and anatomical landmark selection,

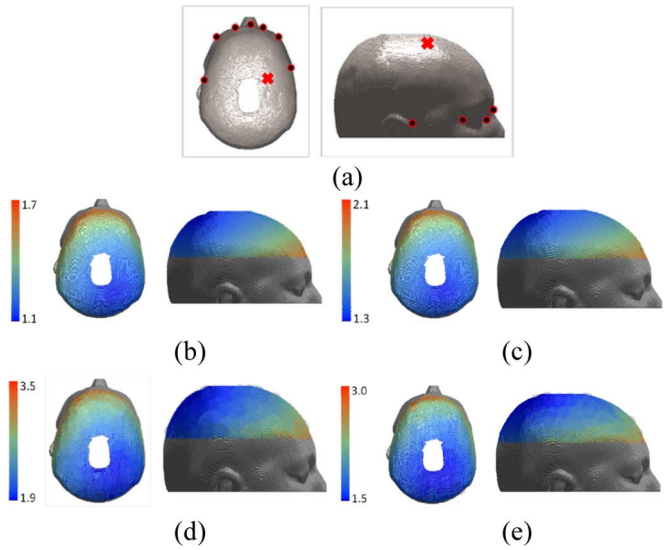

Fig. 9. Estimated color TRE maps showing the expected error obtained by adding fiducial markers on the surface of the patient's head. (a) Anatomical landmarks and target location. Color maps for the methods: (b) Fitzpatrick *et al.* [6]; (c) Danilchenko *et al.* [12]; (d) simulation-homogeneous FLE distribution, and; (e) simulation-heterogeneous FLE distribution. Color bar units are in millimeters.

three fiducial points configurations were considered and their actual TREs were compared: 1) original predefined anatomical landmarks and a bad fiducial marker placement; 2) original predefined anatomical landmarks and a good fiducial marker placement; and 3) selected optimal anatomical landmarks and a good fiducial marker placement. The anatomical landmarks were selected automatically using our program on the preoperative image of the last five patients. The ETRE values of all possible subsets of anatomical landmarks were computed with the simulation method described in Section IV and the subset with the smallest ETRE value was considered optimal.

Overall, 324 different fiducial pairings were generated and analyzed from three different fiducial configurations, based on 3–6 repetitive selections of the same landmarks on five patients' MRI images and physical anatomy by two surgeons. We measured and compared the actual TRE values, and report the mean, standard deviation, and maximum values for each of the five patients ($324 = \sum_{p=1}^{5} 3 \times 2 \times r_I(p) \times r_W(p)$), where p is the patient number and $r_I(p)$ and $r_W(p)$ are the number of repetitive selections of same landmarks on patient p image and physical world, respectively.

In addition, we compared recommended marker placements and generated a color map of the estimated TRE values on the outer head surface for four different TRE estimation methods, each yielding a different FLE model for one patient, one target, and fixed seven facial anatomical landmarks [Fig. 9(a)].

We also examined the relationship between measured TRE values and the distance between the target and fiducial points center of mass. It was observed that when the FLE is homogeneous, isotropic, and unbiased, the TRE decreases as the center of fiducial points is closer to the target [9]. We examine this relation in the clinical setup with anisotropic and heterogeneous FLE.

TABLE IV
COMPARISON OF FIDUCIAL CONFIGURATIONS

FIDUCIAL CONFIGURATION		Patient 1	Patient 2	Patient 3	Patient 4	Patient 5	All Patients
1. Bad marker + all anatomical landmarks	mean	6.2	5.2	4.3	3.4	6.0	4.7
	std	0.4	0.8	0.8	0.8	0.7	1.3
	max	6.9	6.8	5.5	5.4	7.6	7.6
2. Good marker + all anatomical landmarks	mean	5.3	4.0	4.0	1.8	4.2	3.5
	std	0.5	0.5	0.7	0.4	0.5	1.4
	max	6.0	5.12	5.1	2.8	5.2	6.0
3. Good marker + selected anatomical landmarks	mean	3.6	4.0	4.0	1.8	4.2	3.2
	std	0.6	0.5	0.7	0.4	0.5	1.1
	max	4.7	5.12	5.1	2.8	5.2	5.2

Three fiducial configurations are compared with respect to their measured TRE: 1) 'bad' fiducial marker and all predefined anatomical landmarks; 2) 'good' fiducial marker and all predefined anatomical landmarks, and; 3) 'good' fiducial marker and selected optimal anatomical landmarks. A total of 324 different fiducial pairings were analyzed from three different fiducial configurations, with the 3-6 repetitive selections of the same fiducials on 5 patients' MRI images, and physical anatomy selection by two surgeons. All measured TRE values are reported in mm.

Results: Table IV shows the mean, standard deviation, and maximum actual TRE values for the 324 different fiducial pairings for each of the five patients. The mean observed TRE with the "bad" fiducial marker and all the predefined anatomical landmarks was 4.7 ± 1.3 mm, with a 95% confidence interval of 6.7 mm, and maximum error of 7.6 mm. The mean TRE with the "good" fiducial marker and all the predefined anatomical landmarks was 3.5 ± 1.4 mm, with a 95% confidence interval of 5.7 mm, and maximum error of 6.0 mm. The mean observed TRE with the "good" fiducial marker and selected anatomical landmarks was 3.2 ± 1.1 mm, with a 95% confidence interval of 4.8 mm, and maximum error of 5.2 mm. The mean difference between the TRE of the "bad" and "good" fiducial markers was 1.2 ± 1.0 mm with a maximum improvement of 4.1 mm. The mean difference between the TRE of the "bad" and "good" fiducial marker with optimal anatomical landmarks selection was 1.5 ± 1.0 mm with maximum improvement of 4.1 mm.

Fig. 2 shows that ETRE values are locally continuous and have small variability for small fiducial marker location changes. This indicates that sparse surface sampling used in our method for optimizing multiple fiducial markers placements should not significantly change the optimization result.

Fig. 9 compares recommended marker placements for the four different TRE estimation methods, each assuming a different FLE model for one patient, one target, and seven fixed facial anatomical landmarks [Fig. 9(a)]. In the examined setup, we observe that the estimated TRE values do differ from one method to another, but the estimated TRE maps have similar color coding, and thus yield similar optimal fiducial marker locations [Fig. 9(a)–(d)]. We conclude from this study that the TRE estimation method and the assumed FLE distribution may have minor effect on optimal marker placement.

The correlation between the measured TRE and the distance between the target location and fiducial points center of mass were $\rho = 0.7 (p < 0.001)$ for patient 1, $\rho = 0.39 (p = 0.02)$ for patient 2, $\rho = 0.4 (p = 0.01)$ for patient 3, $\rho = 0.8 (p < 0.001)$ for patient 4, and $\rho = 0.22 (p = 0.19)$ for patient 5. Therefore, a statistically significant positive correlation was observed between the measured TRE and the distance between the target location and fiducial points center of mass in most cases.

VII. DISCUSSION

Our results show that optimizing the placement of a single fiducial marker location while keeping the others fixed reduces the TRE by 25% on average, from 4.7 mm to 3.5 mm. Optimal anatomical landmark selection reduced the mean TRE even further, to an average of 3.2 mm, a reduction of 32%. For most patients, the optimal anatomical landmark selection algorithm selected all predefined landmarks. However, in one case (Patient 1) a subset of landmarks significantly reduced the TRE from 5.3 mm to 3.6 mm. These findings are in contrast with those of West *et al.* [9], and with the common belief that more fiducials reduce the TRE. One possible reason for this discrepancy is that in the analysis of West *et al.* [9], the TRE was computed assuming an independent, isotropic, homogeneous, unbiased, and normal FLE distribution, while in our clinical setup, the actual FLE was found to be anisotropic, inhomogeneous, and with possible bias. Furthermore, from a close examination of the expected errors reported by the navigation system, we hypothesize that the navigation system relies on a least-squares registration method that minimizes the RMS of fiducial distances, similar to the method used in West *et al.* [9]. It is possible that using a different registration method that incorporates a more realistic FLE distribution model will take advantage of the additional fiducial and will further reduce the actual TRE.

In most of the cases, a statistically significant positive correlation was observed between the measured TRE and the distance between the target location and fiducial points center of mass. This is comparable to the results presented in West *et al.* [9]. Yet, in one case (Patient 5), the correlation was weak and not statistically significant. In this case, placing the fiducials such that their center was closer to the target location did not reduce the TRE. A possible explanation for this result is the heterogeneous, anisotropic, and biased FLE distribution of the actual clinical fiducial localization errors [11], [15].

Another interesting observation is that optimizing placement of one fiducial marker results in a similar improvement to that achieved in previous works by optimizing a larger set of fiducials [9], [25], [27]–[29]. This is somewhat unexpected, since it would seem that the TRE of multiple optimized fiducials will be lower (better) than the TRE of a single optimized fiducial marker. We see four possible reasons for this finding: 1) we compared the TRE associated with the "worst" and the "best" fiducial marker locations, while others compared the random and "best" configurations; 2) our optimization is global and independent of the initial seed configuration, which also determines their final result; 3) our solution allows addition or removal of anatomical landmarks based on a TRE estimation method that incorporates a heterogeneous FLE model that is better correlated with actual TRE differences; 4) our simulations use clinical data that includes actual localization errors that occur in the operating room—thus, there is more room for improvement.

An accurate and reliable TRE estimation can provide a great assistance for the surgeon in evaluating the surgery risk and its possible outcome. The TRE methods used in this paper (Fig. 6) may indeed depend on the clinical setup and may be inaccurate and unsafe for this purpose. The clinical validation of TRE estimation methods is a topic unto itself and remains an open problem.

As can be seen in Fig. 6, the analytic methods for TRE estimation yield a mixture of two populations—each one seems to be highly correlated with the actual TRE. One possible explanation for this result is that when the configuration of the points used for registration is similar, the analytic methods become correlated with the actual TRE. Since we have compared registration with same anatomical landmarks and one fiducial located at a good location versus one fiducial at a bad location, two populations that are highly correlated with the actual TRE may be observed.

VIII. Conclusion

This paper presents three new methods for the optimal selection of anatomical landmarks and optimal placement of fiducial markers in image-guided neurosurgery that minimize the TRE. The improvement in accuracy is expected to reduce complications and may enable new procedures that were not possible with suboptimal targeting accuracy.

The proposed methods have several key advantages. Before preoperative image acquisition, they allows automatic computation of the optimal fiducial marker placement and anatomical landmark selection using earlier diagnostic MRI/CT studies. Since these diagnostic images are acquired routinely, no additional patient scanning is required. Regardless of the TRE estimation method, the estimated TRE map provides visual, intuitive feedback of the targeting error, and thus enables the surgeon to relocate fiducial markers and evaluate the expected targeting errors. All TRE estimation methods resulted in a high correlation between estimated and actual TRE differences (Fig. 7). That is, when one configuration was associated with lower estimated TRE, then the actual TRE was also lower in most cases. Since the anatomical landmark selection process is fully automatic, this takes the guesswork out of the registration process and can thus shorten preoperative or intraoperative setup time.

Our results indicate that, with our methods, the estimated TRE can be used to reduce actual TRE measured intraoperatively by fiducial points optimization, with little variation with respect to TRE and FLE models. Note also that rigid registration based on least-squares pairwise distance minimization, the most widely used method nowadays, provides a sound base for our approach. While other registration methods can be considered, we believe that this is a secondary issue for this paper that deserves further investigation on its own in a wider context.

Our methods may be further improved with recently suggested registration and TRE estimation methods that incorporate more realistic FLE models [30], [31]. We believe that our approach can achieve the most accurate targeting localization in neurosurgical navigation without additional hardware. In a clinical experiment optimizing placement of one fiducial marker and anatomical landmarks selection we have observed an average TRE improvement of 1.5 mm. TRE improvement can allow safer and more accurate minimally invasive neurosurgical procedures.

Acknowledgment

The authors would like to thank S. Fraifeld for her assistance and for revising this paper.

References

[1] J. M. Fitzpatrick, "The role of registration in accurate surgical guidance," *Proc. Inst. Mech. Eng. Part H*, vol. 224, pp. 607–622, 2010.

[2] T. Peters and K. Cleary, *Image-Guided Interventions: Technology and Applications*. New York: Springer, 2008.

[3] T. M. Peters, "Image-guidance for surgical procedures," *Phys. Med. Biol.*, vol. 51, pp. R505–R540, 2006.

[4] R. J. Maciunas, "Computer-assisted neurosurgery," *Clin. Neurosurg.*, vol. 53, pp. 267–71, 2006.

[5] G. Eggers, J. Muhling, and R. Marmulla, "Image-to-patient registration techniques in head surgery," *Int. J. Oral Maxillofac. Surg.*, vol. 35, pp. 1081–1095, 2006.

[6] J. M. Fitzpatrick, J. B. West, and C. R. Maurer, Jr., "Predicting error in rigid-body point-based registration," *IEEE Trans. Med. Imag.*, vol. 17, no. 5, pp. 694–702, Oct. 1998.

[7] R. R. Shamir, L. Joskowicz, S. Spektor, and Y. Shoshan, "Target and trajectory clinical application accuracy in neuronavigation," *Neurosurgery*, vol. 68, pp. 95–102, 2011.

[8] R. R. Shamir, L. Joskowicz, S. Spektor, and Y. Shoshan, "Localization and registration accuracy in image guided neurosurgery: A clinical study," *Int. J. Comput. Assist. Radiol. Surg.*, vol. 4, pp. 45–52, 2009.

[9] J. B. West, J. M. Fitzpatrick, S. A. Toms, C. R. Maurer, Jr., and R. J. Maciunas, "Fiducial point placement and the accuracy of point-based, rigid body registration," *Neurosurgery*, vol. 48, pp. 810–816, 2001.

[10] C. R. Maurer, Jr., J. M. Fitzpatrick, M. Y. Wang, R. L. Galloway, Jr., R. J. Maciunas, and G. S. Allen, "Registration of head volume images using implantable fiducial markers," *IEEE Trans. Med. Imag.*, vol. 16, no. 4, pp. 447–462, Aug. 1997.

[11] R. R. Shamir and L. Joskowicz, "Geometrical analysis of registration errors in point-based rigid-body registration using invariants," *Med. Image Anal.*, vol. 15, pp. 85–95, 2011.

[12] A. Danilchenko and J. M. Fitzpatrick, "General approach to first-order error prediction in rigid point registration," *IEEE Trans. Med. Imag.*, vol. 30, no. 3, pp. 679–693, Mar. 2011.

[13] R. R. Shamir and L. Joskowicz, "Worst-case analysis of target localization errors in fiducial-based rigid body registration," in *Proc. SPIE Med. Imag.*, 2009, vol. 7258, p. 725938.

[14] J. M. Fitzpatrick, "Fiducial registration error and target registration error are uncorrelated," in *Proc. SPIE Med. Imag.*, 2009, vol. 7261, p. 726102.

[15] M. H. Moghari and P. Abolmaesumi, "Understanding the effect of bias in fiducial localization error on point-based rigid-body registration," *IEEE Trans. Med. Imag.*, vol. 29, no. 10, pp. 1730–1738, Oct. 2010.

[16] B. Ma, M. H. Moghari, R. E. Ellis, and P. Abolmaesumi, "Estimation of optimal fiducial target registration error in the presence of heteroscedastic noise," *IEEE Trans. Med. Imag.*, vol. 29, no. 3, pp. 708–723, Mar. 2010.

[17] M. H. Moghari and P. Abolmaesumi, "Distribution of target registration error for anisotropic and inhomogeneous fiducial localization error," *IEEE Trans. Med. Imag.*, vol. 28, no. 6, pp. 799–813, Jun. 2009.

[18] A. D. Wiles, A. Likholyot, D. D. Frantz, and T. M. Peters, "A statistical model for point-based target registration error with anisotropic fiducial localizer error," *IEEE Trans. Med. Imag.*, vol. 27, no. 3, pp. 378–390, Mar. 2008.

[19] M. H. Moghari, B. Ma, and P. Abolmaesumi, "A theoretical comparison of different target registration error estimators," *Med. Image Comput. Comput. Assist. Interv. (MICCAI'2008)*, vol. 11, pp. 1032–1040, 2008.

[20] T. Sielhorst, M. Bauer, O. Wenisch, G. Klinker, and N. Navab, "Online estimation of the target registration error for n-ocular optical tracking systems," *Med. Image Comput. Comput. Assist. Interv., (MICCAI'2007)*, vol. 10, pp. 652–659, 2007.

[21] B. Ma, M. H. Moghari, R. E. Ellis, and P. Abolmaesumi, "On fiducial target registration error in the presence of anisotropic noise," *Med. Image Comput. Comput. Assist. Interv, (MICCAI'2007)*, vol. 10, pp. 628–635, 2007.

[22] J. M. Fitzpatrick and J. B. West, "The distribution of target registration error in rigid-body point-based registration," *IEEE Trans. Med. Imag.*, vol. 20, no. 9, pp. 917–927, Sep. 2001.

[23] R. R. Shamir, L. Joskowicz, and Y. Shoshan, "What is the actual fiducial localization error in image-guided neuronavigation?," *Int. J. CARS*, vol. 5, pp. S107–S108, 2010.

[24] W. Liu, H. Ding, H. Han, Q. Xue, Z. Sun, and G. Wang, "The study of fiducial localization error of image in point-based registration," *Proc. IEEE Eng. Med. Biol. Soc. Conf.*, vol. 2009, pp. 5088–5091, 2009.

[25] M. Wang and Z. Song, "Improving target registration accuracy in image-guided neurosurgery by optimizing the distribution of fiducial points," *Int. J. Med. Robot*, vol. 5, pp. 26–31, 2009.

[26] R. R. Shamir, L. Joskowicz, and Y. Shoshan, "Optimal landmarks selection for minimal target registration error in image-guided neurosurgery," *Proc. SPIE Med. Imag.*, vol. 7261, p. 72612N, 2009.

[27] N. C. Atuegwu and R. L. Galloway, "Sensitivity analysis of fiducial placement on transorbital target registration error," *Int. J. Comput. Assist. Radiol. Surg.*, vol. 2, pp. 397–404, 2008.

[28] M. Riboldi, G. Baroni, M. F. Spadea, B. Tagaste, C. Garibaldi, R. Cambria, R. Orecchia, and A. Pedotti, "Genetic evolutionary taboo search for optimal marker placement in infrared patient setup," *Phys. Med. Biol.*, vol. 52, pp. 5815–5830, 2007.

[29] H. Liu, Y. Yu, M. C. Schell, W. G. O'Dell, R. Ruo, and P. Okunieff, "Optimal marker placement in photogrammetry patient positioning system," *Med. Phys.*, vol. 30, pp. 103–110, 2003.

[30] R. Balachandran and J. M. Fitzpatrick, "Iterative solution for rigid-body point-based registration with anisotropic weighting," in *Proc. SPIE Med. Imag.*, 2009, vol. 7261, p. 72613D.

[31] M. H. Moghari and P. Abolmaesumi, "Point-based rigid-body registration using an unscented kalman filter," *IEEE Trans. Med. Imag.*, vol. 26, no. 12, pp. 1708–1728, Dec. 2007.

[32] R. Balachandran, E. B. Welch, B. M. Dawant, and J. M. Fitzpatrick, "Effect of MR distortion on targeting for deep-brain stimulation," *IEEE Trans. Biomed. Eng.*, vol. 57, no. 7, pp. 1729–1735, Jul. 2010.

[33] A. D. Wiles and T. M. Peters, "Improved statistical TRE model when using a reference frame," *Med. Image Comput. Comput. Assist. Interv. (MICCAI'2007)*, vol. 10, pp. 442–449, 2007.

[34] A. D. Wiles and T. M. Peters, "Real-time estimation of FLE statistics for 3-D tracking with point-based registration," *IEEE Trans. Med. Imag.*, vol. 28, no. 9, pp. 1384–1398, Sep. 2009.

[35] B. K. P. Horn, "Closed-form solution of absolute orientation using unit quaternions," *J. Opt. Soc. Am. A-Optics Image Sci. Vis.*, vol. 4, pp. 629–642, 1987.

[36] R. R. Shamir, M. Freiman, L. Joskowicz, S. Spektor, and Y. Shoshan, "Surface-based facial scan registration in neuronavigation procedures: A clinical study," *J. Neurosurg.*, vol. 111, pp. 1201–1206, 2009.